QCD Low Energy Footprint

Rami Rom[(a)]

Abstract: QCD affects electron and nucleon through the vacuum quark and gluon condensate dynamics. We propose a double well potential model for the electron and pion tetrahedron dynamics on a pion tetrahedron lattice that represents the vacuum, where quarks are exchanged between electron and pion tetrahedron creating effective motion of the electron. Dirac's electron Zitterbewegung frequency, $\frac{2m_e c^2}{\hbar}$, is related herein to the ground state frequency of the proposed double well potential having a barrier height of at least $2m_e c^2$, the threshold for production of an electron-positron pair. The pion tetrahedron density variation in space may be measured using the Zitterbewegung variation between the aphelion and perihelion of earth's elliptic trajectory using Penning-trap technique. Magnetoresistance and spin torque may be explained by a QCD based electron and pion tetrahedron gas model. We suggest adding the pion tetrahedrons condensate energy density to Einstein's equation energy-momentum tensor. We propose that the Zitterbewegung force free trembling motion and the Zero-Point-Energy (ZPE) electromagnetic field fluctuations are low energy QCD tracks of the vacuum pion tetrahedrons.

Keywords: Electron-Ion Collider (EIC), Pion tetrahedrons, Quantum Chromodynamics (QCD) vacuum, Zitterbewegung, Zero-Point-Energy (ZPE), Penning-trap, Magnetic Materials, General Relativity (GR).

(a) Email: romrami@gmail.com

1. The Electron and Pion Tetrahedron Clouds

The Electron-Ion Collider (EIC) will explore the building blocks of matter and the strong force that binds protons and neutrons. The EIC will explore the three-dimensional distributions in coordinate and momentum spaces of the quarks and gluons inside nucleons and the way their mass, spin, and mechanical properties emerge. The EIC program will include exotic meson spectroscopy aimed to observe the exotic meson states[1].

Semiclassical electron models beyond the standard model (SM) having a ring, a torus, or a sphere structure rotating in the speed of light with the zitterbewegung force free trembling motion were reviewed by Santos[2]. In these models the zitterbewegung is considered a real oscillatory motion of the electron. Santos describes the role of the zero-point-energy (ZPE) electromagnetic field fluctuations and the electron mass in terms of a holographic surface-to-volume ratio. Haramein et al proposed a generalized holographic model (GHM), where the origin of the proton mass is the zero-point energy (ZPE) fluctuations. Planck Spherical Units (PSU) oscillations limited by screening surfaces determine the proton mass[3].

However, the GHM does not specify what is the underlying structure that oscillates and form the Planck Spherical Units and similarly the semiclassical electron models described by Santos do not specify what are the sub-particles that form the proposed electron ring/torus/spherical structure.

Herein we propose that the two valence quarks, $u\ and\ d$, and their antiquark pairs, $\tilde{u}\ and\ \tilde{d}$, are the fundamental building blocks. Accordingly, hadrons, leptons and the non-empty QCD vacuum, are all built from these valence quarks and antiquarks building blocks. We propose that the zitterbewegung force free trembling motion[4] and the ZPE fluctuations are low energy QCD tracks of the vacuum pion tetrahedrons.

In previous papers[5,6,7], the exotic meson, $u\tilde{d}d\tilde{u}$, pion tetrahedron and the electron tetrahedron models were presented. We assumed that the exotic meson pion tetrahedron, $u\tilde{d}d\tilde{u}$, fill space and form a non-uniform condensate with an atmospheric like density drop. The pion tetrahedron mass may be calculated by measuring the β decay rate time periodic variability[6]. We further assumed that the attraction between quarks and antiquarks may be the source of gravity[5]. The massive pion tetrahedrons density vary according to the gravitational field in space and the gravitational force is transferred by interaction of quarks with the anti-quarks of the non-uniform pion tetrahedron condensate.

We assumed that the electron may be a comprised particle, a tetraquark tetrahedron, two quarks determine its electric charge, and two quarks determine the electron spin. High frequency quark exchange reactions may transform the electron tetrahedrons to pion tetrahedrons and vice versa and form together electron clouds with fixed spin state[4]. The $u\tilde{u}$ and $d\tilde{d}$ quark pairs assumed to be part of the electron tetrahedrons, allow forming chemical bonds between electron pairs and proton-neutron pairs in the nuclei forming the $u\tilde{d}d\tilde{u}$ pion tetrahedron that act as a QCD glue. We assumed that the valence quarks and antiquarks ($u, d, \tilde{d}$ and $\tilde{u}$) are conserved sub-particles and may only be exchanged between reactants forming products.

In this paper we propose that electron and pion tetrahedrons form electron clouds in thermal equilibrium due to the high frequency quark exchange reactions, we interpret as Dirac's equation zitterbewegung[2], that occur between the electrons and the pion tetrahedrons. We further assume that two electron tetrahedrons scattering with opposite spins creates a pion tetrahedron transition state complex that acts like a QCD glue and dissipates heat to the pion tetrahedron condensate.

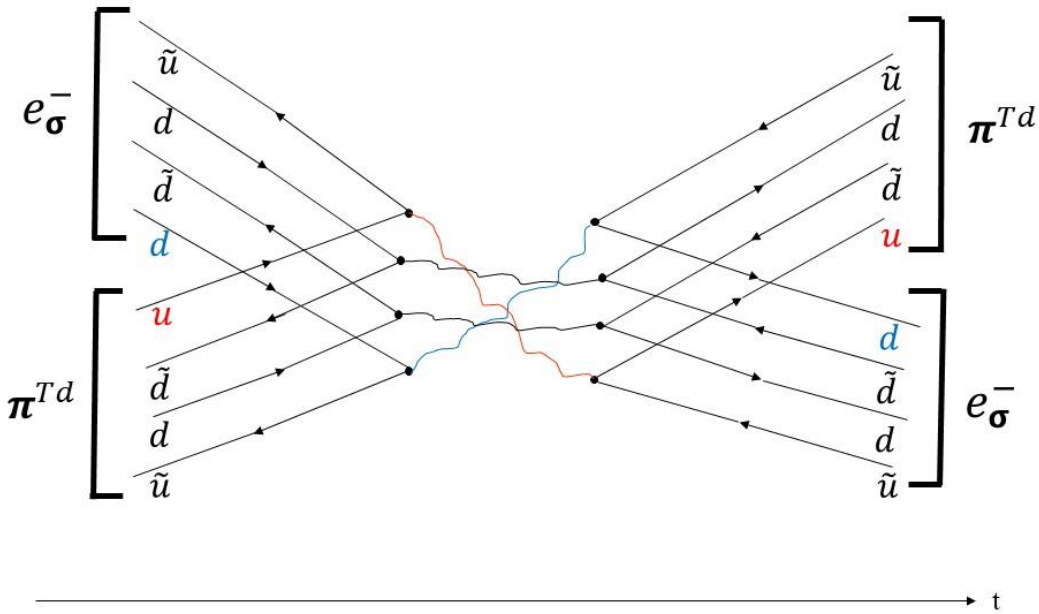

Figure 1 illustrates an electron tetrahedron and pion tetrahedron scattering exchanging d and u quarks, transforming the electron to a pion tetrahedron and vice versa. High frequency quark exchange reactions generate an electron cloud that conserve charge and spin and may be seen as a quark flavor exchange wave with the zitterbewegung frequency ($1.55 * 10^{21}\ sec^{-1}$).

We assume that when an electron is accelerated, the pion tetrahedrons that surround it are accelerated with the electron in thermal equilibrium due to the rapid quark exchanges. The electron cannot be separated from its surrounding pion tetrahedrons cloud, and the electron becomes a many-body cloud composed of millions of pion tetrahedrons that perform rapid d and u quark exchange reactions with the electron tetrahedron. The thermal equilibrium with the pion tetrahedron condensate assumption applies not only to the electrons. Protons and neutrons participate also in the rapid quark exchange reactions with the vacuum pion tetrahedrons. We assume that protons and neutrons of atom nuclei in the solid state are surrounded by the vacuum pion tetrahedrons since the pion tetrahedrons antiquarks are attracted to the quarks of the protons and neutrons. Since the density of matter inside the solid is much higher than in the gas, the non-uniform pion tetrahedron condensate density inside a solid. In the next sections we describe the electron and pion tetrahedrons motion in a lattice in a hydrogen atom model generating the quark flavor exchange waves.

2. Electron and Pion Tetrahedron Cloud and the Hydrogen Atom

Werner Heisenberg introduced in 1925 matrix mechanics trying to explain the electron trajectories $(x(t), p(t))$ for the hydrogen atom in an electromagnetic field arguing that the electrons do not move in classical orbits as Niels Bohr suggested[8]. Quantum mechanics explained electron dynamics in terms of wave functions and discrete energy levels according to equations that were derived a year later by Erwin Schrodinger and in 1928 by Paul Dirac. The wave mechanics gave the correct spectra and the probability to find the electron, but it did not provide a detailed description of the electron motion and an explanation for the zitterbewegung discovered by Schrodinger based on Dirac equation[2].

The hydrogen atom hyperfine structure Hamiltonian may be written in terms of Dirac's exchange operator, $\hat{P}^{Ex}$, the exchange energy parameter A and the Pauli spin matrices for the electron σ^e and the proton σ^p are[9] -

$$\hat{H}^{hyperfine} = A\,\sigma^e\sigma^p = -A\,\sum(2\,\hat{P}^{Ex} - 1) \tag{1}$$

Dirac's exchange operators, $\hat{P}^{Ex}$, exchanges the two particles' spins. If their spins are in the same state, the overall spin state remains unchanged but if their spin states are anti-parallel the two spins are switched.

$$\hat{P}^{Ex}\,|P^{\uparrow}, e^{\uparrow}\rangle = |P^{\uparrow}, e^{\uparrow}\rangle \tag{2a}$$

$$\hat{P}^{Ex}\,|P^{\downarrow}, e^{\uparrow}\rangle = |P^{\uparrow}, e^{\downarrow}\rangle \tag{2b}$$

$$\hat{P}^{Ex}\,|P^{\uparrow}, e^{\downarrow}\rangle = |P^{\downarrow}, e^{\uparrow}\rangle \qquad (2c)$$

$$\hat{P}^{Ex}\,|P^{\downarrow}, e^{\downarrow}\rangle = |P^{\downarrow}, e^{\downarrow}\rangle \qquad (2d)$$

The hyperfine Hamiltonian matrix in the basis set of the four possible spin states, $|P^{\uparrow}, e^{\uparrow}\rangle$, $|P^{\uparrow}, e^{\downarrow}\rangle$, $|P^{\downarrow}, e^{\uparrow}\rangle$, $|P^{\downarrow}, e^{\downarrow}\rangle$ is given by the following 4*4 matrix[10] -

$$\hat{H}_{i,j}^{hyperfine} = \begin{bmatrix} A & 0 & 0 & 0 \\ 0 & -A & 2A & 0 \\ 0 & 2A & -A & 0 \\ 0 & 0 & 0 & A \end{bmatrix} \qquad (3)$$

Solving the time dependent Schrodinger equation for the hyperfine Hamiltonian -

$$i\,\hbar\,\dot{C}_i = \sum_{j=1}^{4} \langle i|\hat{H}_{i,j}^{hyperfine}|j\rangle\ C_j \qquad (4)$$

gives the ground state solution as an antisymmetric combination of the two anti-parallel spin states, $1/\sqrt{2}\ \left(|P^{\uparrow}, e^{\downarrow}\rangle - |P^{\downarrow}, e^{\uparrow}\rangle\right)$, with the ground state energy -3A and the three other states have the same positive energy +A. The total energy difference is $\Delta\mathrm{E}^{\mathrm{hyperfine}} = 4A$. The hyperfine energy split is the source for the 21 cm line emission by hydrogen atom clouds in space of $5.87\ 10^{-6}$ eV. The hyperfine energy split is six orders of magnitude smaller than the difference between the hydrogen electronic ground state $E_{n=1}^{hydrogen}$ and its first excited states $E_{n=2}^{hydrogen}$, which is 10.2 eV. Dirac's spin exchange operator $\hat{P}^{Ex}$ are used also in spin lattice models to exchange spins of two adjacent lattice sites generating spin waves[8] with energies $\hbar\omega_k = 2A(1-\cos(kb))$, where for small k values, kb << 1, equals to $\hbar\omega_k = Ak^2b^2$ and an effective mass may be calculated.

The two aspects, i.e. the hyperfine energy split and spin waves are adapted below for the description of the hydrogen atom surrounded by a pion tetrahedrons lattice. We propose that electron dynamics may be explained by rapid quark exchange reactions that occur between the electrons and the pion tetrahedrons we describe as quark and antiquark flavor exchange waves in analogy to spin waves we relate to the electron zitterbewegung. Accordingly, QCD affects electron motion in atoms via the vacuum pion tetrahedron condensate.

We assumed in a previous paper that the electron tetrahedrons have two quark compositions that determine their spin state[5]. One electron tetrahedron has the quark composition $d\tilde{u}\,\tilde{d}d$ (spin up configuration) and the second electron tetrahedron quark composition is $d\tilde{u}\,\tilde{u}u$ (spin down configuration). The two electron tetrahedrons are surrounded by the vacuum pion tetrahedrons $\tilde{u}d\tilde{d}u$ forming together electrons clouds in thermal equilibrium. The exchanged quarks for the spin up electrons are the d and u quarks, while the exchanged quarks for the spin down electrons are the $\tilde{u}$ and $\tilde{d}$ quarks.

We adapt here the spin lattice model for the QCD vacuum and assume that each lattice site contains a pion tetrahedron or an electron tetrahedron. The transition between the two occurs by exchanging a d quark with a u quark or a $\tilde{d}$ and a $\tilde{u}$ quarks as shown in figure 2a below. Similar quark exchange reactions can be illustrated for spin up and spin down positrons exchanging d and u quarks or $\tilde{u}$ and $\tilde{d}$ anti-quarks as shown in figure 2b.

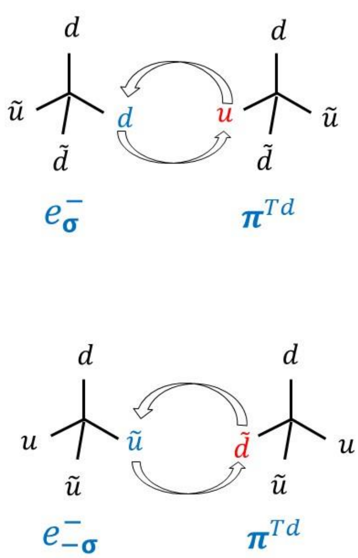

Figure 2a illustrates quark exchange reactions for the spin up and the spin down electrons with pion tetrahedrons. The exchanged quarks for the spin up electron are the d and u quarks, while the exchanged quarks for the spin down electron are the $\tilde{u}$ and the $\tilde{d}$ anti-quarks.

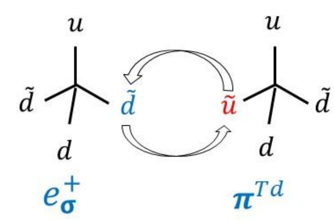

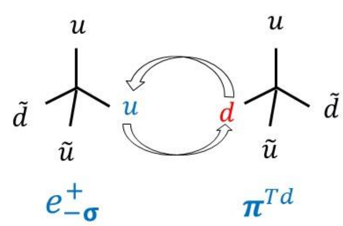

Figure 2b illustrates quark exchange reactions for the spin up and the spin down positrons with pion tetrahedrons.

The quark flavor exchange reactions may occur in two neighboring lattice sites and can also occur between two distant lattice sites, i and j, with a probability $P_{i,j}$.

For the hydrogen atom model, we propose a pion tetrahedron lattice with two co-centric spheres. In each lattice site there is a pion tetrahedron $|\pi_i^{Td}\rangle = |\tilde{u}d\tilde{d}u\rangle_i$ except for one site that contains an electron tetrahedron that we assume may have two possible configurations, a spin up electron configuration $|e_j^{\uparrow}\rangle = |\tilde{u}d\tilde{d}d\rangle_j$ or a spin down electron configuration $|e_j^{\downarrow}\rangle = |\tilde{u}d\tilde{u}u\rangle_j$. Four states characterized by the underlying quark flavor exchange waves in the two co-centric spheres may exist according to which quarks are exchanged, the quarks or the anti-quarks in each sphere domain.

The two quark flavor exchange reactions are -

$$\tilde{u}d\tilde{d}u\,(\pi^{Td})_i + \tilde{u}d\tilde{d}d\,(e^{\uparrow})_j \rightarrow \tilde{u}d\tilde{d}d\,(e^{\uparrow})_i + \tilde{u}d\tilde{d}u\,(\pi^{Td})_j \quad (5)$$

$$\tilde{u}d\tilde{d}u\,(\pi^{Td})_i + \tilde{u}d\tilde{u}u\,(e^{\downarrow})_j \rightarrow \tilde{u}d\tilde{u}u\,(e^{\downarrow})_i + \tilde{u}d\tilde{u}u\,(\pi^{Td})_j \quad (6)$$

Where in the first quark flavor exchange reaction the u and d quarks are exchanged (equation 5) and in the second the $\tilde{u}$ and $\tilde{d}$ quarks are exchanged (equation 6). The four states possible for the two co-centric spheres are:

(u, d) flavor exchange in the inner sphere and (u, d) flavor exchange in the outer sphere,

(u, d) flavor exchange in the inner sphere and ($\tilde{u}$, $\tilde{d}$) flavor exchange in the outer sphere,

($\tilde{u}$, $\tilde{d}$) flavor exchange in the inner sphere and (u, d) flavor exchange in the outer sphere and

($\tilde{u}$, $\tilde{d}$) flavor exchange in the inner sphere and ($\tilde{u}$, $\tilde{d}$) flavor exchange in the outer sphere.

In each of the quark flavor exchange reaction, the electron spin is conserved as equation 5 and 6 show. Interaction with the proton spin may flip the electron spin according to equation 7 below that we assume may occur on the surface between the two spheres for the electron. For the proton, the spin flip requires the exchange of a $\tilde{u}u$ meson with a $\tilde{d}d$ meson or vice versa.

$$uud\tilde{u}u\,(P^{\downarrow})_i + \tilde{u}d\tilde{d}d\,(e^{\uparrow})_j \rightarrow uuddd\,(P^{\uparrow})_i + \tilde{u}d\tilde{u}u\,(e^{\uparrow})_j \quad (7)$$

We note that the valence quarks and anti-quarks numbers are conserved by equation 7 and also that the proton's mass is higher than the mass of its three valence quarks, uud, where the extra mass is typically explained by additional gluons and possibly virtual mesons like the $\tilde{u}u$ and $\tilde{d}d$. The nucleon structure and spin are main research topics of the EIC[1]. We assume here that the proton contains additional $\tilde{u}u$ or $\tilde{d}d$ mesons that determine the proton spin states.

After the two spins are flipped, the quark flavor exchange wave can continue propagating according to equation 5 or 6 above in each sphere domain. We assume that if the proton and electron spins are anti-parallel, the electron crosses the sphere surface smoothly with no need for a spin flip that cost in additional energy. The anti-parallel spin states are favorable and have lower energy. The four possible states of the two domains are shown below in figure 3. The first domain is the inner sphere with a radius a_s and the second domain is the outer sphere with Bohr radius a_0.

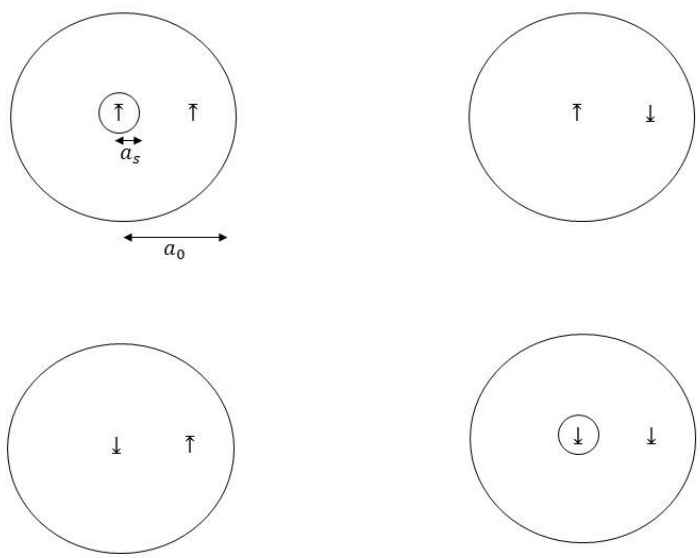

Figure 3 illustrates the hydrogen atom model with two co-centric pion tetrahedron spheres where the quark flavor exchange waves occur in separated domains or a single domain.

With the proposed model, the hyperfine energy split may be explained by the quark flavor exchange wave domains. With anti-parallel spins, there is only one domain with a larger volume for the quark or antiquark flavor exchange waves. If the two spins are parallel, two separated quark flavor exchange wave domains are created, and the configuration has higher energy.

We can estimate the radius of the internal domain sphere, a_s , using the measured hydrogen atom hyperfine energy split of $5.87\ 10^{-6}$ eV and then calculate the quark flavor exchange wave energy density ρ_E for the hydrogen atom electron and pion tetrahedron cloud lattice model

$$\Delta E^{\mathrm{hyperfine}} = \frac{4}{3}\,\pi\, a_0{}^3\rho_E - \left(\frac{4}{3}\,\pi\, a_0{}^3 - \frac{4}{3}\,\pi\, a_s{}^3\right)\rho_E = \frac{4}{3}\,\pi\, a_s{}^3\,\rho_E \qquad (8)$$

$$E_2^{hydrogen} - E_1^{hydrogen} = \frac{4}{3}\,\pi\,(a_{n=2})^3\,\rho_E - \frac{4}{3}\,\pi\,(a_{n=1})^3\rho_E \qquad (9)$$

The ratio of the hyperfine energy and the difference between the hydrogen ground state (n=1) and the first excited states (n=2) is independent of the energy density ρ_E that allows calculating the internal sphere radius a_s −

$$\frac{\Delta E^{hyperfine}}{E_2^{hydrogen} - E_1^{hydrogen}} = \frac{5.87\ 10^{-6}}{10.2} = \frac{a_s{}^3}{a_{n=2}{}^3 - a_{n=1}{}^3}\ ; \quad a_{n=2} = 4\,a_{n=2},\ a_{n=1} = 0.529^{-10} \qquad (10)$$

Accordingly, the radius of the inner domain, a_s, is $6.346^{-13}m$ and the ratio of a_s and a_0 (Bohr radius) is

$$\frac{a_s}{a_0} = \frac{6.346 * 10^{-13}}{0.529 * 10^{-10}} = 0.01199 \qquad (11)$$

Next, we can calculate the quark flavor exchange wave energy density ρ_E for the ground state of the hydrogen atom electron and pion tetrahedron cloud lattice using equation 8

$$\rho_E = \frac{\Delta E^{\mathrm{hyperfine}}}{\frac{4}{3}\pi\, a_s{}^3} = \frac{5.87 * 10^{-6}\ 1.60218 * 10^{-19}}{\frac{4}{3}\pi (6.346 * 10^{-13})^3}\ \frac{\mathrm{jouls}}{m^3} = 8.785 * 10^{11}\ \frac{\mathrm{jouls}}{m^3} \qquad (12)$$

The quark flavor exchange wave energy density ρ_E in units of eV per atom is -

$$\rho_E = \frac{8.785 * 10^{11} * \frac{4}{3}\pi\, a_0{}^3}{1.60218 * 10^{-19}} = 3.4\ \frac{\mathrm{eV}}{atom} \qquad (13)$$

The quark flavor exchange wave energy density per atom, 3.4 eV, contributes about 25% of the hydrogen atom ground state energy of -13.6 eV. If we add the electron rest mass and the internal rotations and vibrations energy of the four pion tetrahedrons quarks in each lattice site as an effective rest mass energy, we may recover another 25% and over all get 50% of the ground state energy as a sum of kinetic and rest mass energies. The remaining 50% of the total ground state energy may be due to the electrostatic Coulomb potential of the proton.

In terms of the relativistic energy-momentum equation

$$E^2 = (pc)^2 + (m_o c^2)^2 \tag{14}$$

We can relate the kinetic energy term, pc, to the electron center of mass motion / drift and the rest mass term $m_o c^2$ with the quark flavor exchange waves on the lattice forming the electron cloud. It should be noted that the proposed vacuum pion tetrahedron lattice cell length may be observed as contracted to a moving electron with a velocity v according to the Lorentz transformation.

$$\Delta x' = \frac{\Delta x}{\Upsilon} \quad ; \quad \Upsilon = \frac{1}{\sqrt{1-(\frac{v}{c})^2}} \tag{15}$$

The motion of the electron from site to site in the lattice may form a ring shape, a helical motion on a torus or a spherical shape like described by Santos[2]. However, in our model, the underlying motion is of the quarks that exchange their flavors on adjacent sites by quantum tunneling via a potential barrier and hence the electron motion does not follow a specific classical trajectory. Since the proposed pion tetrahedron lattice includes in each site a pion tetrahedron boson, $\tilde{u}d\tilde{d}u$, excitations of the lattice may be constrained to have a left or right rotation of the electric field based on the internal motion of the quark charges $\tilde{u}d_{(-q)}$ *and* $\tilde{d}u_{(+q)}$ in each lattice site. The pion tetrahedron lattice may be seen as an electromagnetic medium, where each pion tetrahedron represents a virtual electron-positron pair, and where the motion of massless excitations of the pion tetrahedron lattice may represent photons propagating with the speed of light that do not require exchange of quark flavors as proposed for the electron motion. The photons may be carried by the pion tetrahedrons internal motion vibrations and rotations of the four quarks and antiquarks.

3. Electron and Pion Tetrahedron Lattice and the Zitterbewegung

Using a double well potential Hamiltonian,

$$\hat{H} = \frac{\hat{p}^2}{2m} + m\,\lambda\ (x^2 - a^2)^2 \quad (16)$$

The tunneling probability, T, from the first to the second potential well in the ground state through the potential barrier, $V_0 = m\,\lambda\,a^4$, shown in figure 4 below is[11]

$$T = e^{-\frac{8\,ma^3\sqrt{2\lambda}}{3\hbar}} = e^{-\frac{32V_0}{3\hbar\omega}} \quad (17)$$

ω is the ground state frequency in each well separately given by

$$\omega = \frac{2\pi}{\tau} = \sqrt{8\,\lambda\,a^2} \quad (18)$$

Adapting the double well potential Hamiltonian of equation 16 to the quark flavor-exchange symmetric reaction between electron and a pion tetrahedron in lattice sites i and j (described by equation 5 or 6 above), the velocity of the electron tetrahedron from site i to j due to the flavor exchange wave is calculated by the distance between the sites, 2a, divided by the time period, τ, and multiplied by the tunneling probability in the ground state T.

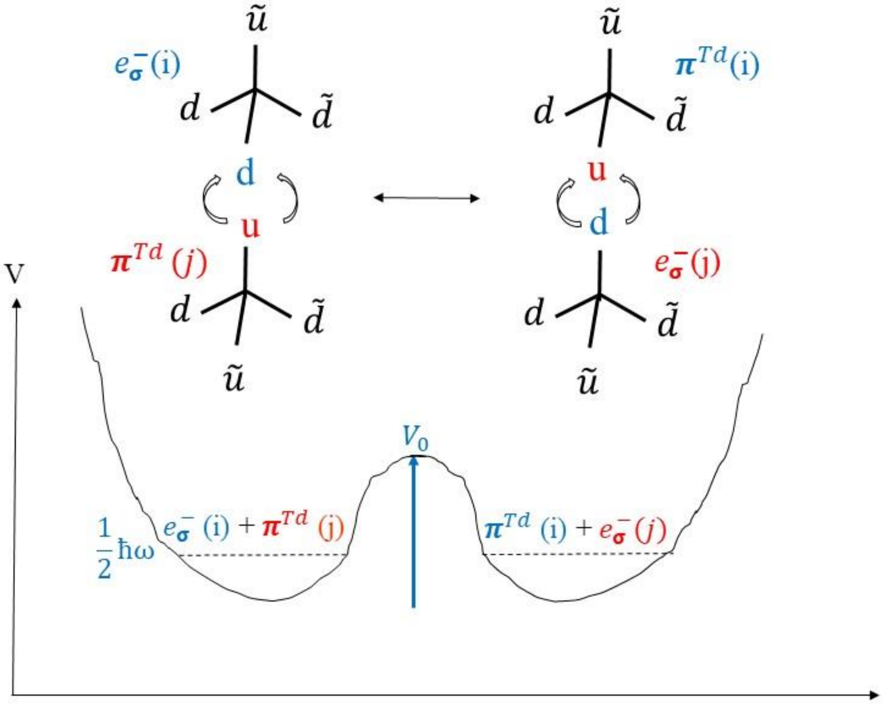

Figure 4 illustrates the double well model for the electron and pion tetrahedron quark flavor exchange reaction in lattice sites i and j in the ground state

We further assume that the potential barrier V_0 may vary in space and determine the electron velocity

$$v_e = \frac{2a}{\tau}\mathrm{T} = \frac{a\omega}{\pi} e^{-\frac{32V_0}{3\hbar\omega}} \tag{19}$$

Assuming that the electron velocity is limited by the speed of light, we get the following expression for the hoping velocity from site to site

$$\frac{a\omega}{\pi} = c\, e^{\frac{32}{3}} \tag{20}$$

$$\frac{v_e}{c} = e^{-\frac{32}{3}\left(\frac{V_0}{\hbar\omega} - 1\right)} \tag{21}$$

The electron does not follow a classical trajectory, quarks are exchanged between the pion tetrahedron sites by tunneling through a potential barrier and effectively create the motion of the electron as a delocalized cloud. We assume that in some small Compton length range, $V_0 = ħ\boldsymbol{\omega}$, and the electron speed is equal to the speed of light as in Dirac's equation zitterbewegung[12]. Out of this small region that may be in a shape of a ring or a torus, $V_0 > ħ\boldsymbol{\omega}$, and the electron speed is smaller than the speed of light. The double well potential barrier height for the quark flavor exchange in lattice sites i and j may be a function of the quark states $V_0\,(d_i, u_j)$. The pion tetrahedron quarks may rotate or vibrate with long range correlations creating local electric and magnetic fields since they are charged.

For example, acceleration by an external electric field will reduce the barrier height in the boost direction. The potential barrier height adaptation may occur with the speed of light and precedes the motion of the slower quark flavor exchange wave. For example using equation 21, with $\frac{V_0}{ħ\omega} = 2.29$ the electron velocity $\frac{v_e}{c}$ is 10^{-6}, with $\frac{V_0}{ħ\omega} = 1.43$ the electron velocity $\frac{v_e}{c}$ is 0.1 and with $\frac{V_0}{ħ\omega} = 1.0001$ the electron velocity $\frac{v_e}{c}$ is 0.999. The double well potential with $\frac{V_0}{ħ\omega} = 1.0$ and with $\frac{V_0}{ħ\omega} = 2.0$ are shown below. With larger potential barrier V_0 value the wells are steeper, the tunneling probability through the barriers is smaller, the quark flavor exchange wave propagation is slower and the electron ground state wavefunction is more localized inside the well.

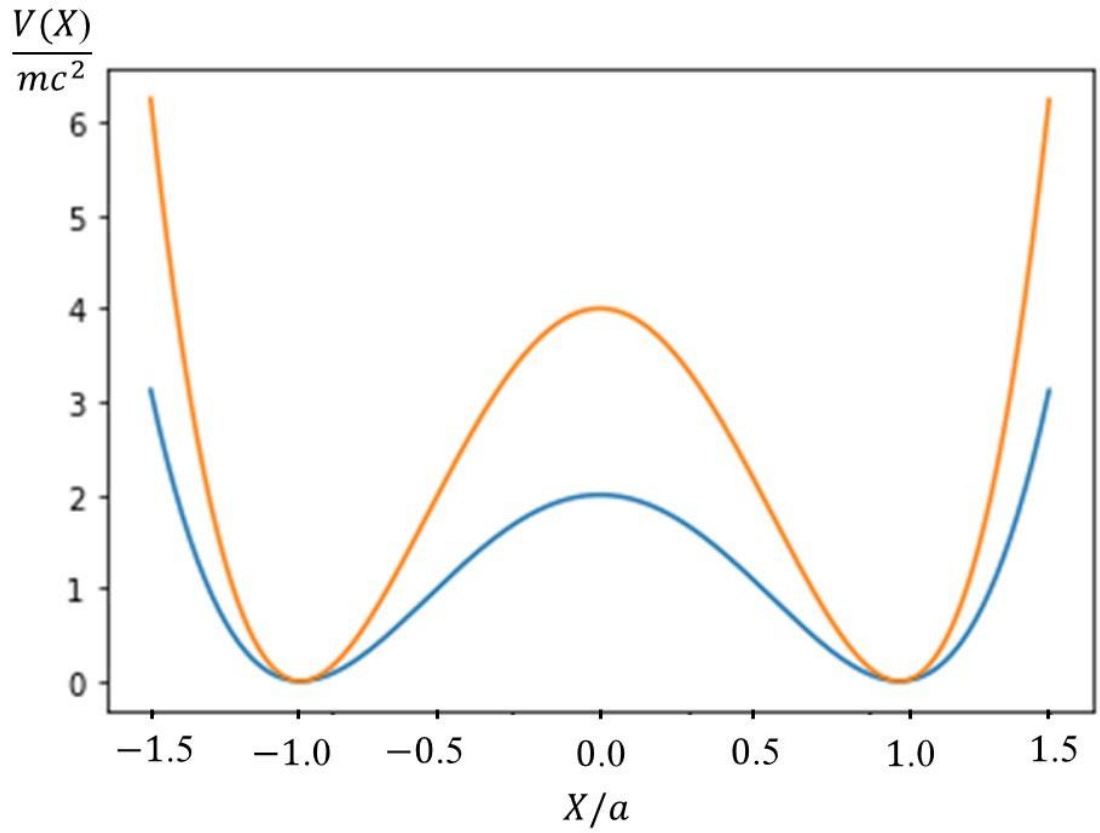

Figure 5 illustrates the double well potential with two values of the barrier height $V_0 = 2m_ec^2$ and $V_0 = 4m_ec^2$ with a = $2.6 * 10^{-8}\ m$.

The hoping frequency ω (equation 20 above) depends on the pion tetrahedron lattice cell length a

$$\omega = \frac{\pi c e^{(\frac{32}{3})}}{a} = \frac{4.040559*10^{13}}{a} \frac{1}{sec} \qquad (22)$$

Using the zitterbewegung frequency, in the Compton region where the potential barrier height is minimal $V_0 = \hbar\boldsymbol{\omega}$, we can calculate the pion tetrahedron lattice cell length in free space

$$\frac{2m_ec^2}{\hbar} = \omega = \frac{4.040559*10^{13}}{a} \frac{1}{sec} \qquad (23)$$

$$a = \frac{4.040559*10^{13}}{1.5527*10^{21}} = 2.60227 * 10^{-8} \text{ meter} \qquad (24)$$

In the Compton region where the potential barrier height is $V_0 = \hbar\boldsymbol{\omega}$, with the zitterbewegung frequency $\omega = \frac{2m_e c^2}{\hbar}$, the barrier height is $V_0 = 2m_e c^2$, which is the threshold for production of an electron-positron pair. The approximate ground state energy inside the well $E_0 = \frac{1}{2}\hbar\boldsymbol{\omega} = m_e c^2 = 5.11 * 10^6\ eV$ is equal to the electron rest mass energy. The potential parameter λ is given by $\lambda = \frac{V_0}{m_e\, a^4} = \frac{2\, c^2}{a^4} = 3.931 * 10^{47} \frac{1}{m^2 sec^2}$

The first order correction to the ground state energy of $\frac{1}{2}\hbar\boldsymbol{\omega}$ in the double well is small[10]

$$E_0^{(1)} = \frac{3\hbar^2}{32 m_e a^2} = 3.38 * 10^{-4}\ eV \qquad (25)$$

Assuming that the mass of the pion tetrahedron is about 6 orders of magnitude smaller than the electron, the pion tetrahedron density in free space may be estimated

$$\rho_{pion\ tetrahedron} = \frac{10^{-6}\, m_e}{(2.6004*10^{-8})^3} = 5.18 * 10^{-14}\ \frac{k_g}{m^3} \qquad (26)$$

The estimated density of the universe is $9.9 * 10^{-27} \frac{k_g}{m^3}$, which is equivalent to 5.9 protons in meter cube. Only 4.7% of the total density is due to visible matter which is about $4.33 * 10^{51} k_g$. The estimated volume of the visible universe is $9.322 * 10^{78} m^3$. If we assume that the pion tetrahedron density in the universe is uniform its mass will be about $4.8 * 10^{65}\ k_g$, 14 orders of magnitude larger than the visible mass. However, we assume that the pion tetrahedron density is dense close to matter particles and is extremely diluted far from matter for example in the cosmic web voids. The pion tetrahedron mass in the universe is probably much smaller than $4.8 * 10^{65}$ k_g, however, due to the huge volume of the universe, the pion tetrahedron mass is probably not negligible.

4. Measuring the Pion Tetrahedrons Density Variation

Using equation 22 above, the density variation of the pion tetrahedron condensate in space may be estimated by measuring the ratio of the zitterbewegung frequency, $\omega = \frac{2m_e c^2}{\hbar}$, in two extreme points of earth's elliptic trajectory around the sun. The ratio of the zitterbewegung frequency will be proportional to the ratio of the electron masses that will be proportional to the inverse ratio of the pion tetrahedron density atmospheric like drop[6].

$$\frac{\omega_{perhelion}}{\omega_{aphelion}} = \frac{m_e^{perhelion}}{m_e^{aphelion}} = \frac{a_{aphelion}}{a_{perihelion}} \qquad (27)$$

The variation of the zitterbewegung frequency may be measured due to the difference in elevation from the sun between the perihelion and the aphelion points of about 5 million km. The zitterbewegung frequency is not directly measurable[2], however, the extremely accurate electron mass measurement using Penning-trap may be sensitive enough to measure the small variations expected[13]. Hence a small deviation from 1 in the electron mass ratio between the perihelion and aphelion will indicate that the vacuum is indeed filled with varying density of pion tetrahedrons that exchange quarks with the proposed non-point like electron tetrahedrons made of quarks.

Expanding the first order correction to the ground state energy with a Taylor series as a function of the pion tetrahedron lattice cell length, we derive an estimate for the expected electron mass variation assuming a 1% variation in the cell length a, $a_{perihelion} - a_{aphelion} \sim 0.01\, a$

$$\frac{\Delta E_0^{(1)}}{c^2} = \frac{3\hbar^2\,(a_{perihelion} - a_{aphelion})}{32 m_e c^2 a^3} = 0.01 \frac{3\hbar^2}{32 m_e c^2 a^2} = 6.01 * 10^{-42}\ \text{Kg} \qquad (28)$$

Since the electron mass is $9.109 * 10^{-31}$ Kg, the measurement accuracy should be of the order of $1.0 * 10^{-11}$. Sturm's Penning-trap technique relative precision of $3.0 * 10^{-11}$ for the electron mass may be sensitive enough[13].

In the next section the magnetoresistance of electrons and pion tetrahedrons in a gas model are described as another example for QCD tracks in low energies.

5. The Electron and Pion Tetrahedron QCD Based Gas Resistance Model

In contrast to most electronic devices and circuits where the electric charge is the main player, magnetic materials use the electron spin to store data and the spin-orbit coupling to switch between the spin states. For example, hard drive discs use magnetic domains formed by typically 10 nanometer size ferromagnetic Co-Pt-Cr grains to maintain stable spin states logical level 0s and 1s. The current that flows through magnetic read head depends on the spin alignment of two ferromagnetic layers that produce the giant magnetic response (GMR) discovered by Fert and Grünberg[14].

Sinova et all described the spin hall effect and Mott’s double scattering spin polarization proposed already in 1929 inspired by Dirac’s electron theory and magnetic tunnel junctions (MTJ)[15,16,17]. First scattering of an electron beam on heavy atom target creates a spin polarized beam that is scattered again by a second heavy atom target creating two currents that can be measured with different chirality.

We propose herein the following electron and pion tetrahedron QCD based gas resistance model that may be used to explains MTJs and Mott’s double scattering and is another example of QCD tracks in low energies. We assume that scattering of two electron tetrahedrons with the same spin that share their pion tetrahedron clouds are elastic collisions with no quark exchange and heat dissipation –

$$\tilde{u}d\tilde{d}d + \tilde{u}d\tilde{d}d \rightarrow \tilde{u}d\tilde{d}d + \tilde{u}d\tilde{d}d \qquad (28a)$$

$$\tilde{u}d\tilde{u}u + \tilde{u}d\tilde{u}u \rightarrow \tilde{u}d\tilde{u}u + \tilde{u}d\tilde{u}u \qquad (28b)$$

However, the scattering of two opposite spin electron tetrahedrons occurs via a pion tetrahedron transition state complex ($\tilde{u}d\tilde{d}d\tilde{u}u\tilde{u}d^{\dagger}, equation\ 29a$) and is an inelastic reaction between the two electron tetrahedrons where quarks are exchanged, heat is dissipated to the pion tetrahedron condensate causing a friction for the electric current flow and switching the electrons' spin as shown in equation 29b (the $\tilde{d}d$ and $\tilde{u}u$ quarks are exchanged) -

$$\tilde{u}d\tilde{d}d + \tilde{u}d\tilde{u}u \rightarrow \tilde{u}d\tilde{d}d\tilde{u}u\tilde{u}d^{\dagger}\ (transition\ state\ complex) \quad (29a)$$

$$\tilde{u}d\tilde{d}d\tilde{u}u\tilde{u}d^{\dagger} \rightarrow \tilde{u}d\tilde{u}u + \tilde{u}d\tilde{d}d \quad (29b)$$

Note that both $\tilde{d}$ and d quarks are exchanged with $\tilde{u}$ and u quarks of the second electron. The quark exchange reaction via the pion tetrahedron transition state complex , $\tilde{u}d\tilde{d}d\tilde{u}u\tilde{u}d^{\dagger}$, cause heat dissipation and electrical resistance that is explained typically by scattering of electrons on solid impurities and the nuclei motion (solid-state phonons). The QCD based electron and pion tetrahedron gas model resistance may be an additional spin dependent mechanism. The proposed quark flavor exchange wave model includes a possible spin-spin interaction between electrons and protons (see equation 7 above) that may be equivalent to electrons interactions with the solid-state phonons.

The MTJ read process may be explained in terms of the QCD based electron and pion tetrahedron gas model as follows: the initial non-polarized electron current has equal number of spin up and spin down electron tetrahedrons, $\tilde{u}d\tilde{d}d$ and $\tilde{u}d\tilde{u}u$. The non-polarized current flows through a first ferromagnetic layer we assume is polarized and let's assume occupied mostly by $\tilde{u}d\tilde{d}d$ electron tetrahedrons. The scattering of two electron tetrahedrons of the same spin is elastic while the scattering of opposite spins creates the transition state complex of the two electrons with a pion tetrahedron, $\tilde{u}d\tilde{d}d\tilde{u}u\tilde{u}d^{\dagger}$ "QCD glue", as illustrated in figure 6. The collision process dissipates heat and cause a delay for one electron tetrahedron configuration. The outcome is that the electron current has now higher percentage of $\tilde{u}d\tilde{d}d$ electron tetrahedrons that were elastically scatters with no delay, e.g. the electric beam becomes polarized.

The polarized current enters the second ferromagnetic layer and the outcome will depend on the second ferromagnetic layer spin state. If it is dominated by $\tilde{u}d\tilde{d}d$ electron tetrahedrons, a favorable parallel ferromagnetic layer configuration (P), the quark exchange reactions will be elastic and a strong current will be measured. However, if the second layer magnetization is in anti-parallel configuration (AP), many more spin flips will occur, heat will be dissipated, and the measured current will be smaller, e.g. higher magnetoresistance.

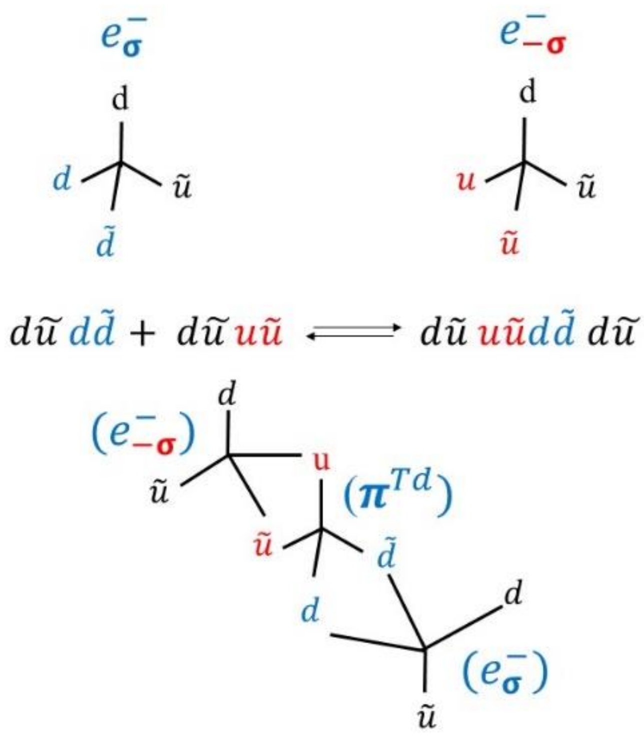

Figure 6 illustrates the pion tetrahedron transition state complex “QCD glue” formed in a collision between two electrons with opposite spins.

The QCD based electron and pion tetrahedron gas resistance model provides a mechanism that may explain why the magnetoresistance of two parallel ferromagnetic layers (P) is lower than the magnetoresistance of the antiparallel (AP) configuration. The pion tetrahedron condensate in the ferromagnetic layer is polarized favorably and allows coherent elastic scattering of electron tetrahedrons with the same spin with no heat dissipation.

The QCD based pion tetrahedron lattice model described above for free electrons and for the hydrogen atom may be expanded to ferromagnets, where multiple electrons share and move on the same pion tetrahedron lattice. Electrons with the same spin are scattered elastically if they collide on adjacent lattice sites, while electrons with opposite spins may create a transition state complex, may exchange their spin state and dissipate heat to the pion tetrahedron lattice by inelastic collisions. Magnetic Random Access Memory (MRAM) is an emerging non-volatile semiconductor memory technology[18] expected to replace traditional computer memory based on complementary metal-oxide semiconductors [19]. MRAM surpasses other types of memory devices in terms of nonvolatility, low energy dissipation and fast switching speed. Future developments in MRAM are based on spin-transfer torque. Spin transfer torque corresponds to the interaction of a spin polarized electronic current with the local magnetization. Magnetic moment is transferred from the conduction electrons to the magnetization resulting in a change of the magnetization orientation[20,21].

MRAM cells include a magnetic tunnel junction (MTJ) that provides the write, read and bit storing functionality, essentially using two magnetic layers, reference layer (RL) and the free layer (FL), separated by a magnesium oxide (MgO) tunnel barrier. The two-bit storage states are the parallel (P) and antiparallel (AP) magnetization orientations[22,23]. Topological insulators provide spin polarized current surface states due to the topology of the bulk band structure[24]. The interplay of electron transport and spin dynamics provide a method to electrical control the magnetization state in Weyl semimetals[25].

According to the QCD based electron and pion tetrahedron gas resistance model described here, we propose a mechanism for the spin torque, where the spin switching in the magnetic free layer (FL) occurs due to electron tetrahedron scattering quark exchanges via the pion tetrahedron transition state complex $\tilde{u}d\tilde{d}d\tilde{u}u\tilde{u}d^{\dagger}$ as shown in figure 6 above and figure 7 below.

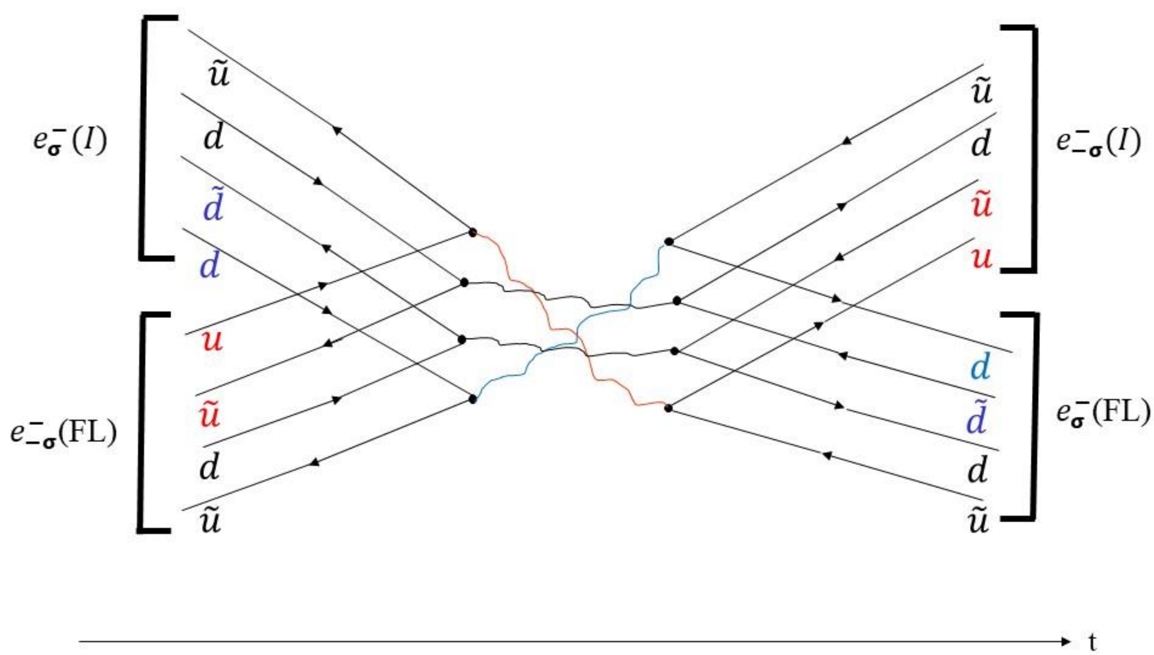

Figure 7 illustrates spin transfer torque by electron-electron scattering, where the upper electron represents a beam of spin polarized electrons $e^-_{\sigma}(I)$ that flows through a free magnetic layer (FL) and are scattered by the FL electrons $e^-_{-\sigma}$(FL) via a pion tetrahedron transition state complex that decays and flip the electrons' spins.

The upper electron represents a beam of spin polarized electrons $e^-_{\sigma}(I)$ that flows through a free magnetic layer (FL) and are scattered by the FL electrons $e^-_{-\sigma}$(FL) that we assume have an opposite magnetization state (AP). The two electron tetrahedrons exchange two quarks via the pion tetrahedron transition state complex and both plip their spin states. Assuming the initial spin state of the free layer was anti-parallel configuration (AP), $e^-_{-\sigma}$(FL), after the scattering its spin is flipped up e^-_{σ}(FL) while the spin of the incoming polarized electrons $e^-_{\sigma}(I)$ that created the spin transfer torque is switched to the down state $e^-_{-\sigma}(I)$. The FL magnetization state is switched from $e^-_{-\sigma}$(FL) to e^-_{σ}(FL). $\tilde{d}$ and d quarks need to be exchanged with the $\tilde{u}$ and u quarks for the proposed spin exchanges.

A competing resilience reaction against switching the magnetization state of the whole magnetic domain will occur on the lattice where adjacent ferromagnetic electrons with opposite spins via the surrounding pion condensate will try to flip back the torqued spin.

$$\tilde{u}d\tilde{u}u(e^-_{-\sigma}) + \tilde{u}d\tilde{d}d(e^-_{\sigma}) \rightarrow \tilde{u}d\tilde{d}d\tilde{u}u\tilde{u}d^{\dagger} \quad (30a)$$

$$\tilde{u}d\tilde{d}d\tilde{u}u\tilde{u}d^{\dagger} \rightarrow \tilde{u}d\tilde{u}u(e^-_{\sigma}) + \tilde{u}d\tilde{d}d(e^-_{-\sigma}) \quad (30b)$$

However, if the torque of the incoming electric current is strong enough above a threshold, an inversion of the magnetic domain will occur and the opposite spin electrons will be pushed out from the inverted magnetic domain. Kateel et al[26] showed that shaping the SOT channel to create a bend below the MTJ device causes an efficient and deterministic inversion of the spin of the FL magnetic domain.

Note that the double quark flavor exchange reaction creates a pion tetrahedron transition state complex "QCD glue" that dissipate heat to the pion tetrahedron condensate and may create a small motion of the pion tetrahedron lattice that are probably extremely small and negligible in low densities and energies. However, in an extremely high-density regions and events, like a black hole or a neutron star mergers, the induced motion of the pion tetrahedron lattice may create gravitation waves that will propagate in the pion tetrahedron lattice.

The pion tetrahedron condensate quark flavor exchange wave energy density in the vacuum is small, however, on cosmological scale it may be significant. In the next section we propose that the vacuum pion tetrahedrons condensate, which is a non-matter component, should be added to Einstein's energy-momentum tensor $T^{\mu\nu}$.

6. The Pion Tetrahedrons and Friedmann Equation

Let's imagine a virtual box in intergalactic space that has a very low density of free electron and pion tetrahedron gas and equal density of protons and neutrons gas for neutrality. Next, let's increase the box such that it includes for example the Milky way galaxy with all its visible mass $M_{Milkyway}$ and in it its center the supermassive Sagittarius A black hole with its mass $M_{Sgr\ A}$.

The Einstein-Hilbert action with a cosmological constant Λ is[27,28,29] -

$$I = \int d^4x \sqrt{-g}\ (\frac{R - 2\Lambda}{16\pi G} + L_M) \qquad (31)$$

Where L_M is the matter Lagrangian. Einstein's field equation is obtained by the requirement that the action will be an extremum with respect to variation of the metric tensor $\delta g^{\mu\nu}$-

$$R^{\mu\nu} - \frac{1}{2} R g^{\mu\nu} + \Lambda g^{\mu\nu} = 8\pi G\, T^{\mu\nu} \qquad (32)$$

The energy-momentum tensor $T^{\mu\nu}$ is given by -

$$T^{\mu\nu} = (\rho + \mathrm{p})\, u_\mu u_\nu + \mathrm{p}\, g^{\mu\nu} \qquad (33)$$

Where u_μ is the tangent velocity 4-vector, ρ is the matter-energy density and p is the pressure.

$$\rho = \frac{M_{matter}}{V} + \frac{M_{black\ holes}}{V} + \rho_{EM} \qquad (34)$$

The matter-energy density includes the matter and black hole mass densities and the electromagnetic energy density of the Milky-way galaxy. The vacuum pion tetrahedrons are not regular matter particles since they are composed of equal parts of matter and antimatter quarks and anti-quarks, however, since pion tetrahedrons are expected to be massive and to exchange quarks with matter particles[2] they contribute energy to Einstein's equation energy-momentum tensor $T^{\mu\nu}$. The pion tetrahedron density $\frac{M_{\pi Td}}{V} = < \Psi_u^\dagger \Psi_d^\dagger \Psi_{\tilde{u}} \Psi_{\tilde{d}} >_\pi$ represents the pion tetrahedron tetraquarks, $\tilde{u}d\tilde{d}u$, condensate. $\Psi_u^\dagger$ is the up quark creation operator, $\Psi_d^\dagger$ is the down quark creation operator, $\Psi_{\tilde{u}}$ and $\Psi_{\tilde{d}}$ are the anti-up and anti-down quark creation operators.

Using the state equation, $p = w\rho$, with $w = -1$, for the expanding universe and Friedmann equation with k=1[27], the following expression for the matter-energy is obtained -

$$H(t)^2 = \frac{\dot{a}^2}{a^2} = \frac{8\pi G}{3}\,\rho + \frac{\Lambda}{3} + \frac{1}{a^2} \tag{35}$$

The matter-energy density ρ is given in terms of the other variables as -

$$\rho = \frac{3\left(H(t)^2 - \frac{\Lambda}{3} + \frac{1}{a^2}\right)}{8\pi G} \tag{36}$$

We propose to calculate the pion tetrahedron condensate density $\frac{M_{\pi Td}}{V}$ as the difference assuming all other variables are known.

$$\frac{M_{\pi Td}}{V} = \frac{3\left(H(t)^2 - \frac{\Lambda}{3} + \frac{1}{a^2}\right)}{8\pi G} - \left[\frac{M_{matter}}{V} + \frac{M_{black\ holes}}{V} + \rho_{EM}\right] \tag{37}$$

A more direct method for calculating the pion tetrahedron mass is based on measurements of the time periodic variability of the $\boldsymbol{\beta}$ decay half-life times of radioactive nuclei's in the perihelion and aphelion of earth's trajectory around the sun[5].

On cosmological scale and due to the huge intergalactic voids, the pion tetrahedron condensate energy density contribution to Einstein's energy-momentum tensor and Friedmann equation may be significant. The pion tetrahedron density is expected to be non-uniform and have an atmospheric like drop far from galaxy centers[4]. However, the pion tetrahedrons are bosons that may be duplicated exponentially by Corley and Jacobson's black hole laser effect[30] in supermassive black holes. The pion tetrahedron density growth and the separation of matter and antimatter particles next to black hole event horizons may increase the energy density and pressure expanding the universe without adding dark matter and energy, where the additional antimatter may be trapped under the event horizon of the supermassive black holes[31].

The pion tetrahedron condensate may be the QCD non-empty vacuum that carry QED, QCD and gravitational forces and it may play the role of the missing dark matter and dark energy. The Zitterbewegung force free trembling motion and the Zero-Point-Energy (ZPE) electromagnetic field fluctuations may be the low energy QCD tracks of the vacuum pion tetrahedrons.

References

[1] Burkert, V.D. et al, (2022), "Precision Studies of QCD in the Low Energy Domain of the EIC", https://www.researchgate.net/publication/365850432_Precision_Studies_of_QCD_in_the_Low_Energy_Domain_of_the_EIC

[2] Santos, I. U., (2023), "The zitterbewegung electron puzzle", https://www.researchgate.net/publication/374257062_The_zitterbewegung_electron_puzzle

[3] Haramein, N., Guermonprez, C., Alirol, O., (2023), "The Origin of Mass and the Nature of Gravity", https://zenodo.org/records/10125315

[4] LeBlanc, L. J. et al, (2013), "Direct observation of zitterbewegung in a Bose–Einstein condensate", https://arxiv.org/abs/1303.0914

[5] Rom, R., (Apr, 2024), "Non-Uniform Pion Tetrahedron Aether and Electron Tetrahedron Model", Journal of High Energy Physics, Gravitation and Cosmology. https://www.scirp.org/journal/paperinformation?paperid=132602

[6] Rom, R., (Apr 2023), "The Quantum Chromodynamics Gas Density Drop and the General Theory of Relativity Ether", Journal of High Energy Physics, Gravitation and Cosmology, 9, No. 2. https://www.scirp.org/journal/paperinformation.aspx?paperid=124153

[7] Rom, R., (Jan 2024), "The Pionic Deuterium and the Pion Tetrahedron Vacuum Polarization", Journal of High Energy Physics, Gravitation and Cosmology, 10, No. 1. https://www.scirp.org/journal/paperinformation?paperid=130928

[8] Rovelli, C., (2021),"Helgoland: Making Sense of the Quantum Revolution", https://www.amazon.com/Helgoland-Making-Sense-Quantum-Revolution/dp/0593328884

[9] Feynman, R., (1965), "The Hyperfine splitting in Hydrogen (lecture on the hydrogen atom ground level spin states)", https://www.feynmanlectures.caltech.edu/III_12.html

[10] Feynman, R., (1965), "The Independent Particle Approximation (lecture on spin waves)",

https://www.feynmanlectures.caltech.edu/III_15.html

[11] Grabovsky, D, (2021), "The Double Well", https://web.physics.ucsb.edu/~davidgrabovsky/files-teaching/Double%20Well%20Solutions.pdf

[12] Davis, B.S., (2020), "Zitterbewegung and the Charge of an Electron",

https://arxiv.org/abs/2006.16003

[13] Sturm, S., et al, (2014), "*High-precision measurement of the atomic mass of the electron"*, https://arxiv.org/abs/1406.5590

[14] Fert, A., Grünberg, P., "*for the discovery of Giant Magnetoresistance, Nobel Prize 2007*", https://www.nobelprize.org/prizes/physics/2007/press-release/

[15] Sinova, J. et al, (2014), "Spin Hall effect", https://arxiv.org/pdf/1411.3249.pdf

[16] Mott, N. F., (1929), Proc. R. Soc. A Math. Phys. Eng. Sci. 124 (794), 425.

[17] Mott, N. F., (1932), Proc. R. Soc. A Math. Phys. Eng. Sci. 135(827), 429.

[18] Apalkov. D., Dieny, B., Slaughter, J.M., (2016), "Magnetoresistive Random Access Memory", **https://ieeexplore.ieee.org/document/7555318**

[19] Dieny, B., Goldfarb, R.B., Lee, K., (2016), "Introduction to Magnetic Random-Access Memory, https://www.wiley.com/en-us/Introduction+to+Magnetic+Random+Access+Memory-p-9781119009740

[20] Baraduc, C., Chshiev, M., Ebels, U., (2009), "Introduction to spin transfer torque", https://www.spintec.fr/introduction-to-spin-transfer-torque/

[21] Ralph, D.C., Stiles, M.D., (2009), "Spin Transfer Torques", https://arxiv.org/abs/0711.4608

[22] Santos, T.S., S., Mihajlovi´c, G., Smith, N., Carey, M., Katin, J.A., Terris, B.D., "Ultra thin perpendicular free layers for lowering the switching current in STT-MRAM", https://arxiv.org/pdf/2008.01343.pdf

[23] Mihajlovi´c, G., Smith, N., Santos, T., Li, J., Tran, M., Carey, M., Terris, B.D., Katine, J.A, "Origin of the resistance-area product dependence of spin transfer torque switching in perpendicular magnetic random access memory cells", https://arxiv.org/pdf/1905.02673.pdf

[24] Yan, B., Felser, C., (2016), "Topological Materials: Weyl Semimetals", https://arxiv.org/abs/1611.04182

[25] Kurebayashi, D., Nomura, K., (2017), "Microscopic theory of electrically induced spin torques in magnetic Weyl semimetals", https://arxiv.org/pdf/1702.04918.pdf

[26] Kateel, V. et al, (2023), "Field-Free Spin-Orbit Torque driven Switching of Perpendicular Magnetic Tunnel Junction through Bending Current", https://pubs.acs.org/doi/10.1021/acs.nanolett.3c00639, https://arxiv.org/pdf/2305.03961.pdf,

[27] Byers, N., (1998), "E. Noether's Discovery of the Deep Connection Between Symmetries and Conservation Laws", https://arxiv.org/abs/physics/9807044

[28] Bak, D., Cangemi, D., Jackiw, R., (1993), "Energy-momentum conservation in gravity theories", https://www.researchgate.net/publication/13272303_Energy-momentum_conservation_in_gravity_theories

[29] Ishak, M, (2019), "Testing General Relativity in Cosmology", https://www.researchgate.net/publication/329770055_Testing_general_relativity_in_cosmology

[30] Corley, S., Jacobson, T., (1999) , "Black Hole Lasers", https://arxiv.org/pdf/hep-th/9806203.pdf

[31] Rom, R., (Apr 2023), "Matter Reactors", Journal of High Energy Physics, Gravitation and Cosmology, 9, No. 2. https://www.scirp.org/journal/paperinformation.aspx?paperid=124154